

STANDARD MODEL GROUP, QCD SUBGROUP - DYNAMICS
ISOLATING AND TESTING THE ELEMENTARY QCD SUBPROCESS*

Michael J. Tannenbaum
Brookhaven National Laboratory, Upton, New York 11973

Introduction

QCD to an experimentalist is the theory of interactions of quarks and gluons. Experimentalists like QCD because QCD is analogous to QED. Thus, following Drell and others¹ who have for many years studied the validity of QED, one has a ready-made menu for tests of QCD. There are the static and long distance tests such as:

- the value of the coupling constant α_s
- the shape of the QCD potential and "onia" spectroscopy in analogy to atomic spectroscopy and tests of Coulomb's law at large distances. (One might try to imagine the QCD analogue of g-2 and the Lamb shift.)
- tests of confinement: i.e., can you break up a proton into 3 quarks?

These topics are covered by Peter LePage in the static properties group. In this report, dynamic and short distance tests of QCD will be discussed, primarily via reactions with large transverse momenta.

This report is an introduction and overview of the subject, to serve as a framework for other reports from the subgroup. In the last two sections, the author has taken the opportunity to discuss his own ideas and opinions. Other people who contributed to the QCD dynamics subgroup were:

- a. ep - Structure Functions:
J. Friedman, W. Lee, T. O'Halloran,
G. Tzanakos, D.H. White
- b. ep, e⁺e⁻ - Jets in Final States
M. Derrick, J. Friedman, H. Sticker
- c. e⁺e⁻ - QCD Tests in Resonance Decays
M. Tuts, H. Vogel
- d. Exclusive Reactions
G. Bunce
- e. Hadron-Hadron
R.L. Cool, R. Odorico, H. Sticker,
M.J. Tannenbaum

The basic equations for the elementary QCD constituent subprocesses have been given by Cutler & Sivers² and by Combridge, Kripfganz & Ranft.³ These are what I call "pure" QCD processes, only involving quarks and gluons, and are shown in Figure 1. Most of these processes follow directly from analogy with QED and one can recognize Moller, Bhabha and Compton scattering. However, the distinctive feature of QCD compared to QED is that gluons carry color charge whereas photons do not carry electric charge. This is illustrated by the diagrams in the dashed box which involve the gluon self coupling and have no analogy in QED.

* Work performed under the auspices of the U.S. Dept. of Energy.

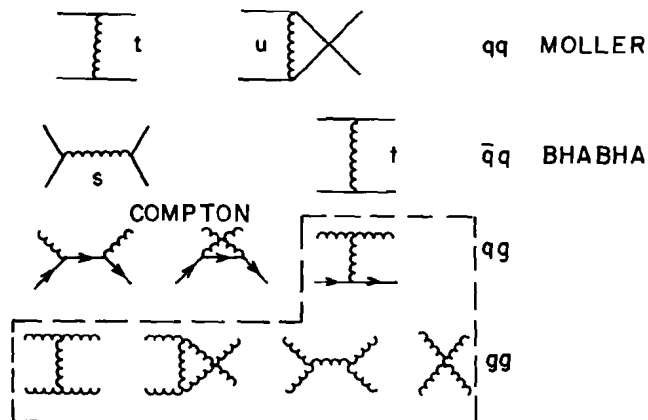


FIGURE 1

Another distinctive feature of QCD is that the coupling constant α_s changes with the momentum transfer, Q^2 , of the reaction, with a scale parameter Λ . In a model with four flavors:

$$\alpha_s(Q^2) = 12\pi/25 \ln(Q^2/\Lambda^2) .$$

The scattering cross sections for the constituent subprocesses are given by the formula:

$$\frac{d\sigma}{dt} = \frac{\pi\alpha_s^2(Q^2)}{s^2} \times \int (\cos \theta^*) \quad (1)$$

where s, t, and u are the Mandelstam variables of the subprocess; s = the total constituent c.m. energy squared; t = the invariant four-momentum-squared of the scattering, and s + t + u = 0. It is worthwhile to recall that in terms of the constituent subprocess scattering angle, θ^* :

$$\begin{aligned} t &= -s \frac{(1 - \cos \theta^*)}{2} \\ u &= -s \frac{(1 + \cos \theta^*)}{2} \end{aligned} \quad (2)$$

and the constituent transverse momentum is

$$P_T = \sqrt{s} \frac{\sin \theta^*}{2} .$$

For 90° scattering

$$2 P_T = \sqrt{s} \quad (3)$$

and

$$u = t = -2 P_T^2 .$$

The angular factors $\int (\cos \theta^*)$ are given in Table I³ for the pure QCD processes of Figure 1.

One of the conceptual difficulties in dealing with QCD compared to QED is that experiments can not be performed directly on quarks and gluons. Thus a "standard" methodology has developed as illustrated for proton-proton collisions. The protons consist of 3 valence quarks and gluons which can scatter as constituents but can never emerge as free particles (presumably) because of a conservation law. The scattered

Hard scattering subprocesses in QCD and the associated differential cross-sections in lowest order. Σ is defined by eq. (1). The initial (final) colours and spins have been averaged (summed). q and g denote quark and gluon, respectively. Subscripts 1, 2 denote distinct flavours. s, t, u are the Mandelstam variables of the subprocess.

$q_1 q_2 \rightarrow q_1 q_2,$	$\frac{4}{9} \frac{s^2 + u^2}{t^2}$
$q_1 \bar{q}_2 \rightarrow q_1 \bar{q}_2$	$\frac{4}{9} \frac{s^2 + u^2}{t^2}$
$q_1 q_1 \rightarrow q_1 q_1$	$\frac{4}{9} \left(\frac{s^2 + u^2}{t^2} + \frac{s^2 + t^2}{u^2} \right) - \frac{8}{27} \frac{s^2}{ut}$
$q_1 \bar{q}_1 \rightarrow q_2 \bar{q}_2$	$\frac{4}{9} \frac{t^2 + u^2}{s^2}$
$q_1 \bar{q}_1 \rightarrow q_1 \bar{q}_1$	$\frac{4}{9} \left(\frac{s^2 + u^2}{t^2} + \frac{t^2 + u^2}{s^2} \right) - \frac{8}{27} \frac{u^2}{st}$
$q\bar{q} \rightarrow gg$	$\frac{32}{27} \frac{u^2 + t^2}{ut} - \frac{8}{3} \frac{u^2 + t^2}{s^2}$
$gg \rightarrow q\bar{q}$	$\frac{1}{6} \frac{u^2 + t^2}{ut} - \frac{3}{8} \frac{u^2 + t^2}{s^2}$
$qg \rightarrow qg$	$-\frac{4}{9} \frac{u^2 + s^2}{us} + \frac{u^2 + s^2}{t^2}$
$gg \rightarrow gg$	$\frac{9}{2} \left(3 - \frac{ut}{s^2} - \frac{us}{t^2} - \frac{st}{u^2} \right)$

TABLE I

constituents are thought to materialize as jets of hadrons at large transverse momenta, while the "spectator" quarks and gluons continue in the beam directions and also rematerialize as jets. Thus, the probability of observing a single real particle at large transverse momentum is given by the product of following probabilities:

$$P_1(x_1) \times P_2(x_2) \times \frac{d\sigma}{dt}(s, \cos \theta^*) \times F(z) \quad (4)$$

where $P_1(x_1)$ is the probability of a constituent of proton 1 to have a fraction x_1 of its total momentum, $P_2(x_2)$ is the same thing for the other proton, $d\sigma/dt$ is the constituent scattering probability given by Eq. (1), and $F(z)$ is the probability that the observed particle would have a fraction z of the momentum of the scattered constituent. The total proton-proton c.m. energy-squared is S and the constituent c.m. energy squared is $s = x_1 x_2 S$. The constituent c.m. system is moving with longitudinal momentum P_L in the proton-proton c.m. system, where $2 P_L/S = x_1 - x_2$. The transverse momentum P_T is the same in both systems. Note that all the variables except s^2 in Eq. (1) are dimensionless or "scaling" variables.

As the subject progressed, some inadequacies of Eq. (4) became apparent. The structure functions $P(x)$ and the fragmentation functions $F(z)$ do not scale exactly but evolve with Q^2 in a way that is predictable in QCD. In addition, an initial state transverse momentum k_T must be assigned to the constituents in each proton,⁴⁻⁵ and a fragmentation transverse momentum j_T must be assigned to each jet. Furthermore, it has been observed⁶ that k_T is not a constant but increases with both \sqrt{s} and P_T .

Outline of Dynamic QCD Tests and Main Problems

One can try to categorize the tests of QCD in three main areas as follows:

(1) Can the existence of the QCD subprocesses be proved and their properties measured? Can the basic features of QCD be demonstrated?

- Validity of fancy formulas (see Table I).
- Gluon self-coupling.
- Running of the coupling constant α_s with Q^2 .
- Higher order processes.

(2) Jets: Are they fundamental, or just a nuisance?

- Do QCD jets exist? Measurement of their properties in various reactions.
- Are large E_T jets dominated by hard scattering processes?
- Triggered jet studies. Use high P_T single particle to select hard scattering and look for jets.

(3) Can hard collisions be used a tool?

- Try to knock a real quark out of a hadron.
- Search for quark substructure.
- Exploit flavor independence of QCD to find new particles in fragments of QCD jets.

If it were not for the peculiar nature of QCD in which there is no direct experimental access to the interacting particles, we could concentrate on the fundamental topic 1, and ignore topic 2. Unfortunately, this is not possible. One of the principal obstacles in testing QCD is that external parameters are required in order to unravel the constituent subprocesses. In principle, these parameters should themselves be calculable in QCD, but the subject is still young and developing. In fact, what I call parameters may be more interesting to many physicists than the basic constituent subprocesses.

The parameters which must be understood can be enumerated as follows:

A. Structure Functions

- Quark - traditionally measured in $ep, \nu p$
- Gluon - recently extracted from ν & $\bar{\nu}$ interactions in iron. In principle can be directly measured in the reaction $p+p \rightarrow \gamma^*x$.
- Sea - sensitive to $\nu, \bar{\nu}$ differences and Drell-Yan pair production in pp collisions.
- QCD evolution of structure functions.
- Universality of structure functions - are the structure functions determined by an electroweak probe the same as when measured by a gluon probe? Is the electric charge distribution inside a hadron the same as the color distribution?

B. Fragmentation Functions

- Are they interesting on their own as QCD tests?
- Is there a difference between quark and gluon jets, and different flavor quarks?
- Are flavor and charge of leading particle related to flavor and charge of constituent?

C. Fragmentation Transverse Momentum, j_T , and initial state transverse momentum, k_T .

- How do they enter e^+e^- , ep and hadron-hadron reactions?
- How well can they be measured?
- Are they good tests of QCD in their own right?

D. Higher Twist and other "non-perturbative" effects.

- Decay angular distribution in Drell-Yan pairs from πp .⁷
- Non-factorization of structure and fragmentation functions?

One positive aspect of this large number of parameters is that it has encouraged some experimenters to exercise their art and find creative solutions to testing the underlying QCD subprocesses. Three general classes of attacking this problem have been tried.

Compare Data to All-Encompassing QCD Monte Carlo Program

This was the approach originally taken at Petra⁸ and in the first hadron-hadron calorimeter experiment at Fermilab.⁹ Unfortunately, this approach tends to concentrate more on the details of the assumptions of the Monte Carlo program and less on the actual experimental measurements. It can also lead to the missing of important features of the experimental measurement because they have not been previously understood and incorporated into the Monte Carlo program. For instance, it was at one time thought that high P_T jets in hadron-hadron collisions would be coplanar with the beam direction.¹⁰ However, beautiful work at the CERN-ISR⁴ showed this not be true,¹¹ which caused the incorporation of the k_T parameter.

Measure the Parameters That You Need

The parameters k_T and j_T have been extensively measured in hadron-hadron collisions and in e^+e^- collisions. However, the measurement of many parameters implies significantly increased data taking and running time. Thus, fewer useful data are obtained per unit of integrated luminosity, which implies that much more integrated luminosity is required to obtain a definitive result.

Find Ways to Make Parameter-Independent Quantitative Tests. Find Measurable Quantities Which are Insensitive to the Parameters

Of course, this solution is much more interesting and challenging to experimentalists. In a later section, I will discuss in some detail how this can be done in hadron collisions. However, as pointed out by the Jade¹² and Cello¹³ collaborations and by Field and Wolfram,¹⁴ e^+e^- collisions are not immune to problems B, C, and D. This had been recognized by Soding¹⁵ who reviewed tests of QCD in e^+e^- collisions with emphasis on a parameter-insensitive test which used only the angles between the 3 jets.

A Catalog of the Elementary QCD Subprocesses

Pure QCD Reactions

These are the processes shown in Figure 1 which only involve quarks and gluons: quark-quark, quark-antiquark, quark-gluon, and gluon gluon scattering. These reactions are dominant in hadron-hadron collisions but only appear in very high order in e^+e^- and ep collisions. From Eq. (1), Figure 1 and Table I we see that these processes are sensitive to the gluon self-coupling, the gluon propagator and the running coupling constant $\alpha_s(Q^2)$. Proof of the existence of these subprocesses with properties as predicted would be a major achievement.

Another class of pure QCD subprocesses involving only hadrons is "onia" production in hadron collisions shown in Figure 2 for toponium.¹⁶ This is a gluon fusion process, involving a quark loop, whose cross section and dynamics can be studied in hadron colliders. Parenthetically, one can also try to discover toponium and continue the great tradition of discovering vector mesons (ρ , ω , ϕ , J, T...) in hadron collisions (Figure 3). The subprocess shown in Figure 2 is also responsible for the decay of the "onia". Thus

this purely hadronic subprocess can also be studied in e^+e^- collisions where one can literally sit on s-channel onium resonances.

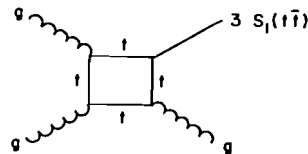


FIGURE 2

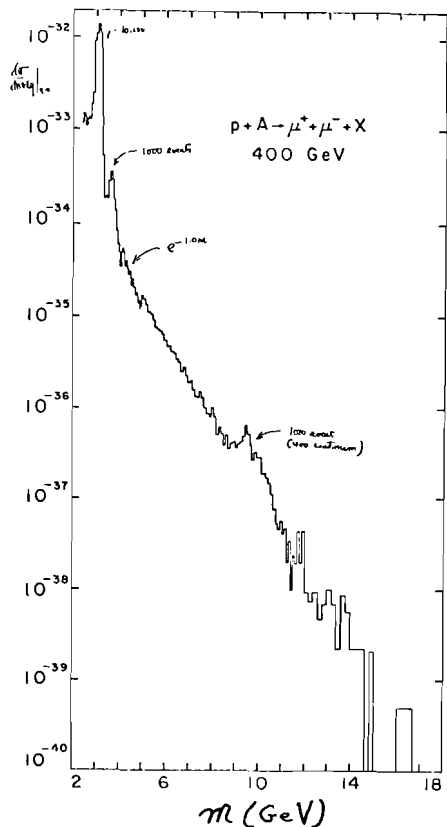


FIGURE 3

While on the subject of these QCD "box" diagrams, an experimentalist may take a flight of fancy and suggest that a good way to study them would be via double onia production (Figure 4). The most reasonable reaction would probably be in double J/ψ production because of the huge lepton-pair branching ratio.

Mixed QCD-QED Reactions

These reactions are accessible at all machines, e^+e^- , ep and pp. The typical processes are shown in Figure 5. The principal process, quark + gluon \rightarrow quark + photon can be studied by direct photon production in pp collisions, and by 3 jet production in e^+e^- and ep collisions. In pp collisions one is directly sensitive to the gluon structure function and the quark propagator; while in e^+e^- and ep one can probe the dynamics of the quark-quark-gluon vertex and test the quark propagator, vector nature of the gluon¹⁷ and the coupling constant.

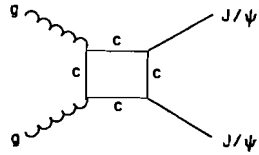
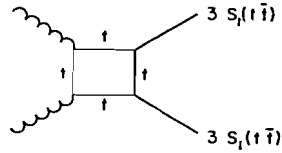


FIGURE 4

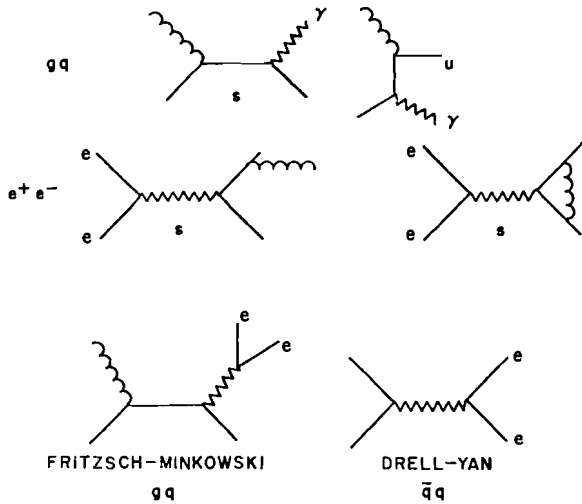


FIGURE 5

Another process is lepton-pair production in hadron collisions which can proceed via the gluon-quark channel (Fritzsch-Minkowski) or $\bar{q}q$ annihilation (Drell-Yan). The analog of Drell-Yan in e^+e^- is simply the total hadronic cross section or R; while in ep it is just the deeply inelastic scattering process, which is still the principal method of determining the nucleon structure functions.

Final states with photons are of particular importance for QCD tests in hadron collisions since the photon interacts at the constituent level but can be directly detected experimentally. The above processes all involve a single photon, either real or virtual, which electromagnetically couples to the constituent quarks. The next higher order QED processes involve two photons which couple to the constituent quarks (Fig. 6).

In hadron collisions, photon-pair production can be caused by the two-photon $q\bar{q}$ annihilation analog of Drell-Yan. This subprocess tests the quark propagator¹⁸ in a way that is reminiscent of "classical" QED tests.¹ It is also the principal subprocesses for the two-photon physics in e^+e^- annihilation, and inelastic Compton scattering in ep.

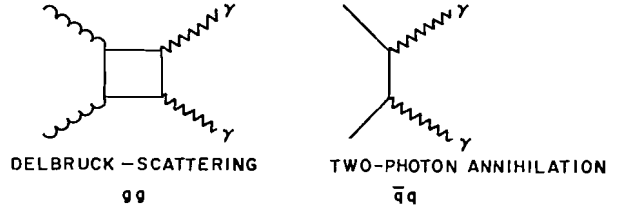


FIGURE 6

A potentially more interesting subprocess is the gluon + gluon \rightarrow photon + photon reaction¹⁹ which proceeds by the box diagram (Figure 6) labelled Delbruck scattering (or more correctly light-by-light scattering). This is a relatively complicated higher order diagram. Proof of the existence of this subprocess with properties as predicted¹⁹ would establish perturbative QCD as a very respectable theory. From the point of view of the naive experimental physicist it seems that double J/ψ production (Fig. 4) in hadron collisions would also be a good test of the box diagram, with a better experimental signature.

Higher Order Processes

The $gg\gamma\gamma$ induced coupling just described is one example of a higher order QCD process. Another example is four (or more) jet production in e^+e^- collisions (or ep or pp). An especially interesting class of higher order processes are those which produce interference effects which must be zero in lowest order. One such effect²⁰ is the linear polarization of direct photons produced in hadron collisions, or equivalently a correlation of the scattering plane to the photon polarization plane in high P_T photoproduction with polarized photons (Figure 7). It is claimed²⁰ that this polarization provides "a rigorous test of perturbative QCD as well as an important check on the color hypothesis". "This latter aspect is particularly attractive because the polarization involves the three-gluon interaction and the equality of the quark-gluon and three-gluon coupling in an essential way."²⁰ Derivatives of this effect are polarization in high P_T lepton pairs (Figure 7), and W^\pm polarization in hadron collisions.²¹

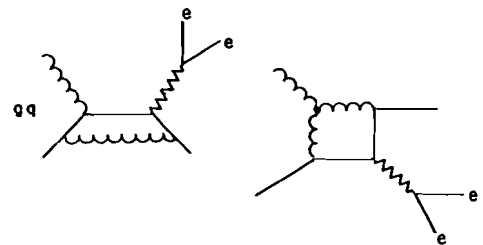


FIGURE 7

Exclusive Processes at Wide Angles

Processes such as elastic scattering and exclusive two-body scattering at large angles also probe QCD subprocesses;²² but in a more complicated way because all the constituents manage to recombine after the interaction. However, these processes have an experimental advantage since all the incoming and outgoing particles are real and can be measured. The main problem is that the cross sections fall very rapidly with increasing energy.

How Experimentalists Try to Attack
The Elusive Constituents

It is clear that the preceding catalog is by no means complete. Nevertheless, it represents quite a tall order. Furthermore, most experimentalists when thinking about QCD dynamics tend to think in terms of the particles they detect, rather than the constituent subprocesses. Thus the experimentalist's arsenal for QCD tests is as follows, with emphasis on hadron-hadron.

a. Single Particle Inclusive Reactions at Various Angles

- high P_T π^0, η^0
- high P_T $\pi^\pm K^+ p$
- high P_T $K^0 \Lambda^0$
- high P_T $K^- \bar{p}$
- high P_T direct γ , real & virtual
- high P_T vector mesons $K^*, \rho^0, \omega^0, \phi^0, \Psi^0, \Upsilon^0, Z^0$, etc.
- all of the above at large x_F , moderate P_T .
- single e^\pm or μ^\pm (τ^\pm)
- D, Λ_c , B, Λ_B production

b. Two Particle Inclusive Reactions

- e^+e^- or $\mu^+\mu^-$ pairs
- $e\mu$ pairs
- pion pairs
- other hadron pairs
- measurement of event structure with 2 particle correlations.

c. Polarization Tests of QCD

- Polarization of inclusive hyperons.
- polarization of direct γ 's
- polarization and parity violation in W^\pm production and decay
- polarization asymmetries with polarized beams, and with polarized beams and polarized targets.

d. Jets

- with single particle triggers
- unbiased jet triggers
- multi-leptons

e. Exclusive Reactions at Large Angles

- elastic scattering
- exclusive 2 body scattering, eg., $\pi^-p \rightarrow K^+\Sigma^-$

The experimentalist's goal is to use the above arsenal to separate or enhance the hard scattering subprocesses and make quantitative measurements. This is an extensive and intricate subject which is reviewed annually at various conferences,²³⁻²⁶ so I shall not attempt to cover it. I have just made a personal selection of a few points to illustrate how it can be done. I have emphasized hadron collisions since many people, unfamiliar with the richness of these interactions, seem to think that they are too dirty for quantitative studies of QCD.

It is Easy to Select Hard Collisions by Triggering on Single Particles at High P_T

Even though these events are rare, the signature is very clean. Furthermore, "trigger bias"²⁷ automatically selects events in the very interesting region of the fragmentation function where the single particle has most of the constituent momentum. Data from the ISR²⁸ show that the average fraction of the jet

momentum taken by a single π^0 trigger, $Z_{trig} = P_T \text{ trigger}/P_T \text{ jet}$, is greater than 80% and is universal as a function of $x_T \equiv 2 P_T/\sqrt{s}$ (Fig. 8).

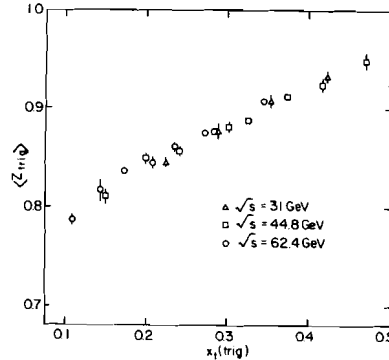


FIGURE 8

Exploit Scaling

Equations (1), (3) and (4) with rigorous scaling imply a single particle inclusive cross section near 90° of the form

$$E d^3\sigma/dP^3 = P_T^{-n} F(x_T) = (\sqrt{s})^{-n} G(x_T), \quad (5)$$

with $n = 4$. Any corrections due to QCD non-scaling effects can be calculated by theorists in analogy to radiative corrections in QED. In fact, the QCD corrected prediction²⁹ is $n \approx 5.5$.

The form of the cross section given by Eq. (5) is particularly easy to analyze. A plot of the invariant cross section $E d^3\sigma/dP^3$ as a function of x_T for different \sqrt{s} should be a series of universal curves with normalization proportional to $(1/\sqrt{s})^n$. This method has the additional advantage that the value of n is insensitive to systematic errors in the absolute P_T scale. This is shown for CCOR ISR data³⁰ in Figure 9. For $x_T > 0.25$, $P_T > 7.5$ GeV/c, the curves for $\sqrt{s} = 53.1$ and 62.4 GeV are indeed parallel and give $n = 5.1 \pm 0.4$. The fit in this region is

$$E d^3\sigma/dP^3 \approx \frac{4 \times 10^{-29} \text{ cm}^2/\text{GeV}^2 \times (1 - x_T)^{12}}{P_T^5} \quad (6)$$

with P_T in GeV/c.

This fit is in quite reasonable agreement with professional QCD predictions when extrapolated up to $\sqrt{s} = 800$ GeV. Figure 10 shows³¹⁻³² Paige's jet cross section Δ , single photon, \circ , and single photon $\rightarrow e^+e^-$ with $1 < M_{ee} < 2$ GeV, \blacksquare . Also shown are Owens, Reya and Gluck's π^0 cross sections, \blacklozenge , which continue neatly onto the fit extrapolation, \bullet , for $P_T > 50$ GeV/c. It would be lovely to have data from a high luminosity collider at ~ 1 TeV and verify that the QCD predictions of Figure 10 do indeed work. An estimate of the first two months single π^0 data at such a collider is shown in Figure 11, assuming the validity of Eq. (6).

The curves are a factor of 2 apart for $n = 5.0$ and would move closer together or farther apart should n be smaller or larger.

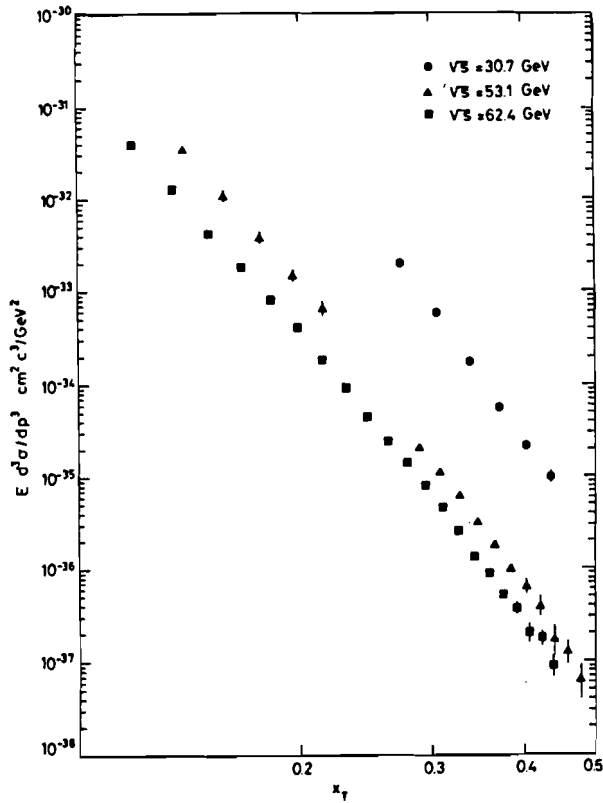


FIGURE 9

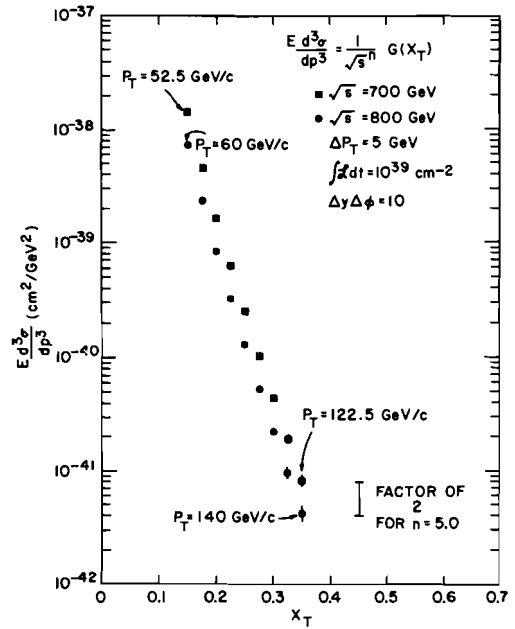


FIGURE 11

Vary P_T , Angle and Particle Detected to Enhance Subprocess

The estimated subprocess composition of inclusive π^0 production at $\sqrt{s} = 800$ GeV is sketched in Figure 12 with apologies to the authors of Ref. 32. The features are only qualitative since the exact form of the gluon structure function, particularly its Q^2 evolution are not well constrained by the data at this time.

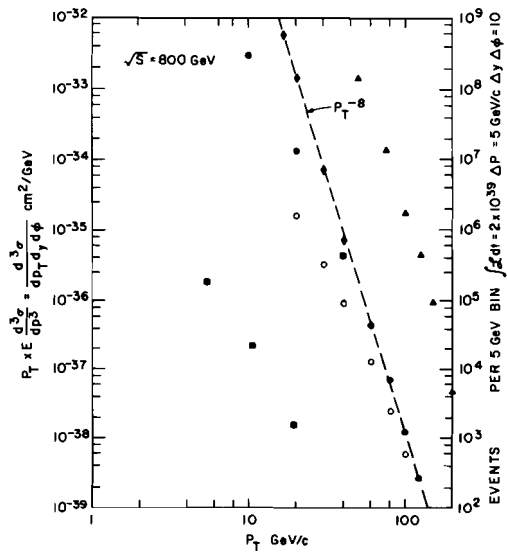


FIGURE 10

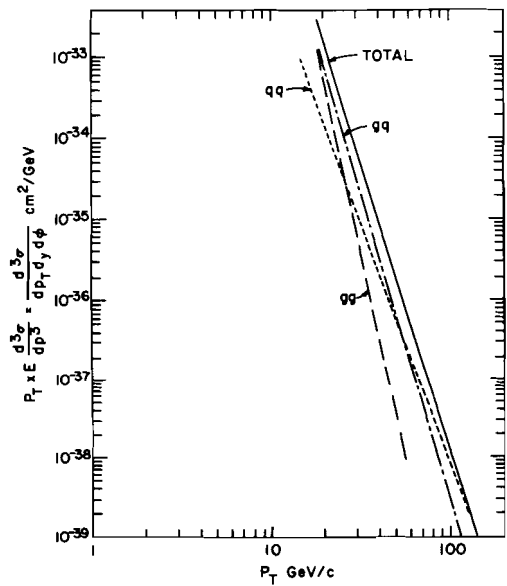


FIGURE 12

Nevertheless since the gluon structure function is softer than the quark structure function, the predictions always have the qualitative feature that at low x_T , gluon-gluon dominates, at medium x_T gluon-quark dominates and at large x_T quark-quark is most important.

While some additional examples of selecting the detected particle to enhance particular subprocesses will be given below, the most striking example is to use high P_T direct γ triggers in hadron collisions to select the QCD compton effect (Fig. 5). A particularly neat example of how this might lead to a precision QCD test was given by R.L. Cool at this meeting.³³

Consider a precision comparison of high P_T direct photon production in pp and $\bar{p}p$ collisions at the same \sqrt{s} . The production mechanisms of single photons in pp and $\bar{p}p$ collisions differ only in that there is a valence anti-quark annihilation contribution in $\bar{p}p$ which becomes dominant over the compton process at large x_T (Figure 13). The structure functions are known and the recoiling jet is a gluon jet in distinction to the recoiling quark jet for the compton process. By measuring the ratio of single photon production to two-photon annihilation (Fig. 6) in $\bar{p}p$ collisions at large x_T one should obtain the ratio³³

$$\frac{\bar{p}p \rightarrow \gamma + \gamma + X}{pp \rightarrow \gamma + X} = \frac{11}{216} \frac{\alpha}{\alpha_s(Q^2)}$$

which might be a precise method to measure α_s .

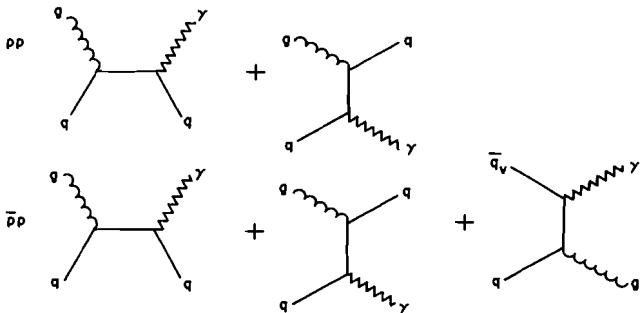


FIGURE 13

One thing that this discussion clearly brings out is the desirability of high luminosity $\bar{p}p$ colliders so that one can get up into the large x_T realm where the effect of the valence anti-quarks in anti-protons can be seen above the gluon "background".

Another neat effect with direct photon production in pp collisions is to measure whether the photons are linearly polarized. This effect,²⁰ as discussed above, is sensitive to the essential features of QCD. There is also a characteristic rapidity dependence. The transverse polarization can be measured as in Figure 7 by using low mass ($1 < M_{ee} < 2$ GeV) pairs and measuring the angular correlation between the production and decay plane of the pair. This is an example of a process where one runs out of rate even at the highest luminosity colliders (Fig. 10). Also the polarization predicted is very small, only at the level of $\sim 2\%$. Note that the analogous polarization effect also occurs in the inverse reaction in ep collisions.³⁴

Further Enhance Subprocess by Using Information from Away Jet or Particles

The use of polar angular correlations has been stressed by the split field magnet group³⁵ at the CERN

ISR as a way to enhance various subprocesses (Figure 14).

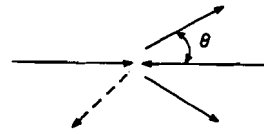


FIGURE 14

The reaction is triggered by a high P_T charged particle at a forward angle $\theta \sim 50^\circ$. If the away jet, or particle, is in the same polar hemisphere (solid arrow), this implies that the constituent c.m. system is moving forward with large $x_F = x_1 - x_2$, so that $x_1 \gg x_2$. Since the quark structure function is much harder than the gluon structure function, the most probable interpretation is that the event was initiated by a quark with large x_1 and a gluon with small x_2 . For away jets, or particles, in the opposite polar hemisphere (dashed arrow), x_F is small, implying $x_1 \approx x_2$, or a symmetric initial state like quark-quark or gluon-gluon. Data and predictions are shown in Figure 15 for R , the ratio of away particles in the opposite polar hemisphere to those in the same polar hemisphere as a function of x_E , which is approximately the ratio of the transverse momentum of the associated particle to that of the trigger.

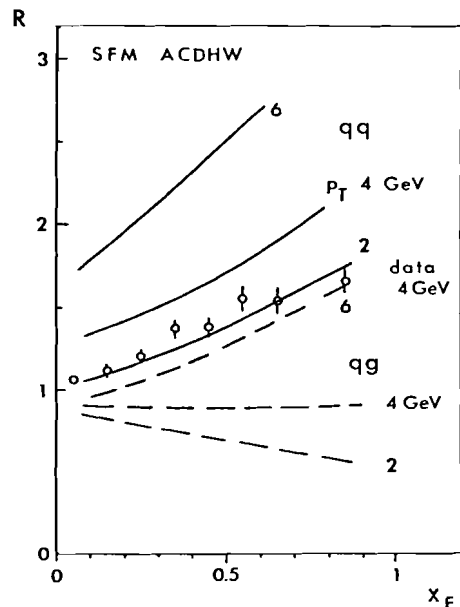


FIGURE 15

Quark-quark always favors the opposite hemisphere by a large margin over quark-gluon, independently of the trigger P_T . The data for $P_T > 4$ GeV seem to indicate roughly equal amounts of each subprocess.

Two-particle azimuthal correlations have been used to map out the structure of events selected by high P_T single particle triggers. The azimuthal distribution of charged particles in the central region ($|y| < 0.7$) is shown⁶ as a function of the charged particle transverse momentum, P_T , for events in which a π^0 is observed with transverse momentum $P_{T\pi^0} > 7$ GeV/c (Figure 16).

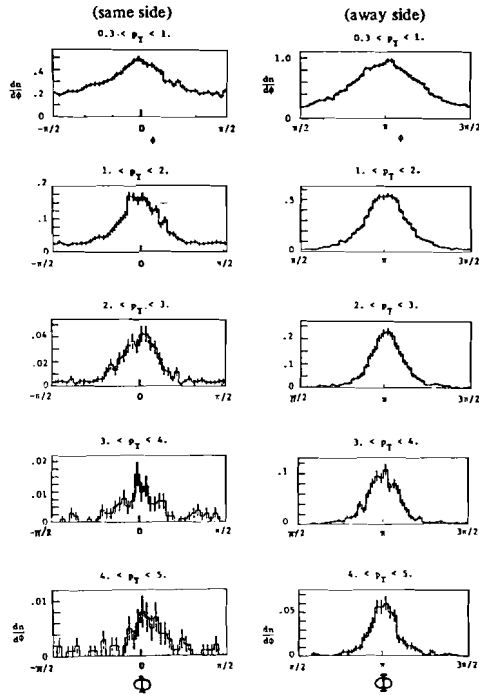


FIGURE 16

A dramatic two-jet structure is evident. There are same(a) and away side(b) azimuthal peaks on top of a "spectator" background of low P_T particles. It is apparently this low P_T background which gives hadron collisions their "dirty" reputation. Evidently, this is a minor problem since the spectator background becomes negligible for particles with transverse momentum $P_T > 1$ GeV/c.

From systematic analyses of the widths of these peaks, the parameters J_T and k_T can be deduced.⁶ Alternatively, the widths of the peaks can be directly analyzed³⁵ in terms of the accoplanarity of the jets which is expected in QCD from initial state gluon emission analogously to the radiative accoplanarity in the reaction $e^+e^- \rightarrow \mu^+\mu^-$.³⁶

Exploit Leading Particles in Jets

Once again, the split field magnet group at the ISR has been a leader here.²⁵ Continuing with the opposite/same polar hemisphere ratio R given above (Fig. 15), they make the same plot for different leading particles (Figure 17).

The data triggered by K^+ and π^+ look quite similar and tend to follow the q - q curve, while the K^- triggers are quite different and follow the q - g curve. Additional systematic studies involving leading particles in jets have led this group to the following rules.^{26,37}

- A leading π^+ selects mainly u -quark jets,
- A leading π^- selects mainly d -quark jets,
- A leading K^- selects mainly gluon jets.

Another approach using leading particles was taken by the CCOR group in π^0 pair data presented at Paris this year.²⁸ Since single particle triggers select events in which the particle has most of the constituent momentum (Figure 8), it stands to reason that in triggers which select two roughly back-to-back particles, both with large transverse momenta, these

leading particles will provide a reasonable representation of the kinematics of the final state constituents (Figure 18).

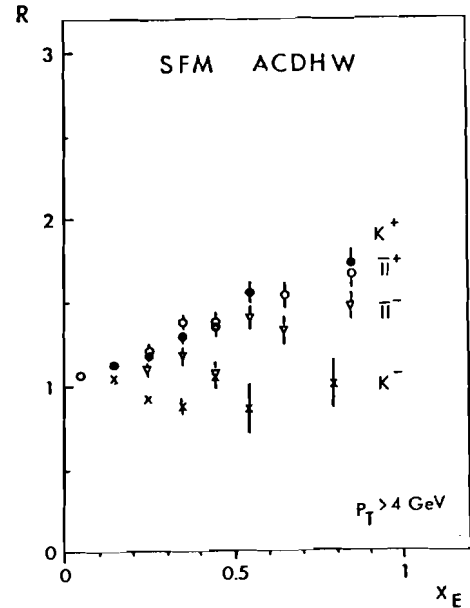


FIGURE 17

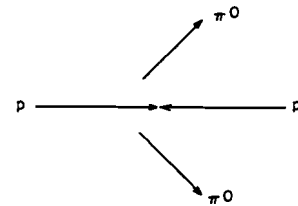


FIGURE 18

In this model, the mass of the π^0 pair will be equal to the constituent cm energy \sqrt{s} , the longitudinal momentum of the pair will give the transformation to the constituent cm system, in which the reaction should look like elastic scattering (Figure 19).

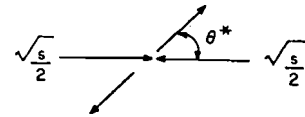


FIGURE 19

The polar angular dependence, $\Sigma(\cos \theta^*)$ (Table I) can then be measured. CCOR obtained the following $\cos \theta^*$ distributions (Figure 20).

The data at $\sqrt{s} = 62.4$ and 44.8 GeV are consistent with being independent of \sqrt{s} and π^0 -pair mass over the range $8 < m_{\pi^0\pi^0} < 16$ GeV; and could be fit with the simple parameterization

$$\Sigma(\cos \theta^*) = \Sigma(0) \times \left[\left(\frac{s}{E} \right)^a + \left(\frac{s}{u} \right)^a \right] \quad (7)$$

with $a = 2.97 \pm 0.05$ and $\chi^2 = 124$ for 116 degrees of freedom. There is also a systematic uncertainty of ± 0.2 .

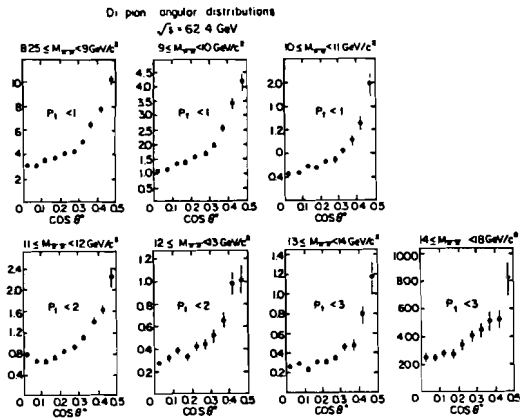


FIGURE 20

The neat part of this analysis is that the measured results can be compared directly to the angular distributions $\Sigma(\cos \theta^*)$ of the QCD constituent subprocesses³ from Table I, as shown in Table II.

Constituent Process Angular Distributions at Fixed s Normalized at 90°

$\cos \theta$	$\alpha_s(\hat{c}) = \text{constant}$				$\left(\frac{g}{g}\right)^2 + \left(\frac{g}{u}\right)^2$	$\left(\frac{g}{g}\right)^3 + \left(\frac{g}{u}\right)^3$	$\frac{q_1 q_1}{s} \times \alpha_s^2(\hat{c})$	$\alpha_s^2(\hat{c})$ $\Lambda = 0.1 \text{ GeV}/c$
	q ₁ q ₁	q ₁ q ₂	qg	gg				
0	1.0	1.0	1.0	1.0	1.0	1.0	1.0	1.0
0.1	1.05	1.04	1.03	1.03	1.03	1.06	1.07	1.02
0.2	1.22	1.17	1.15	1.13	1.13	1.27	1.28	1.05
0.3	1.49	1.43	1.36	1.32	1.32	1.68	1.62	1.085
0.4	2.13	1.88	1.75	1.66	1.64	2.50	2.40	1.125
0.5	3.18	2.69	2.43	2.26	2.22	4.14	3.73	1.174

TABLE II

The agreement is excellent. The gluon-gluon scattering distribution ($\alpha_s = \text{constant}$) is very well parameterized by Eq. (7) with $a = 2$. The fit to the data with $a = 3$ is best represented by identical quark scattering, when the increase in $\alpha_s(Q^2)$ with decreasing $Q^2 \equiv t$ at forward angles is included. Without the variation of α_s with t , the agreement would be considerably worse. The data at face value would appear to exclude gluon-gluon scattering or quark-gluon scattering as significant subprocesses. However the gluon structure function itself evolves strongly as Q^2 is decreased at forward angles, raising the full QCD prediction for the parameter a for gluon-gluon scattering from $a = 2$ to $a = 2.4$ for the $\alpha_s(t)$ variation, and from 2.4 to 2.7 for the structure function evolution.

Large Aperture E_T Triggers

These are an attempt in hadron collisions to try to observe the jet structure of hard collisions directly and in an unbiased way. There are two main problems. The first is that a huge detector with nearly 4π aperture, but with very fine granularity, is required. The second is a physics problem. Large E_T events can be caused by hard collisions but there is also a considerable background in which the large transverse energy is built up from large multiplicity fluctuations, with a large number of particles each having a rather small value of transverse energy.³⁸⁻³⁹

Only this year, have such powerful detectors come into operation. A preview of things to come is given by the spectacular two-jet event at $\sqrt{s} = 540 \text{ GeV}$ obtained by the UA2 collaboration⁴⁰ (Figure 21).

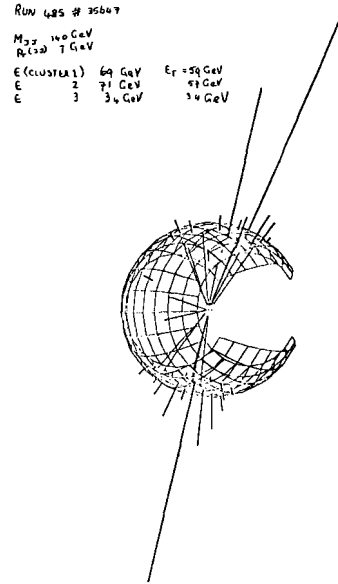


FIGURE 21

It is uncertain whether jet triggers will provide better quantitative tests of QCD than the single particle studies described above; more data are needed. However, it would be an enormous step forward if the huge counting rate advantage of jets over single particles (Fig. 10) could be successfully exploited.

Conclusions

Some conclusions may be drawn from the preceding discussion.

1. Hadron colliders can be exploited to map out pure QCD subprocesses. The structure functions from ep and vp interactions are very helpful in this analysis.
2. Mixed QCD-QED reactions can be measured at all machines. In e^+e^- and ep machines these subprocesses occur only as "radiative" corrections $[1 + \alpha_s(Q^2)]$ to the dominant processes. In hadron collisions they can be isolated via the direct photon final state, which is free of fragmentation uncertainty; however there is a large background from photons from π^0 and η^0 decays.
3. The ISR and Fermilab have been very productive, but $2 P_T \equiv \sqrt{s} \equiv \sqrt{s}/3 \sim 25 \text{ GeV}$ is barely high enough for QCD to dominate. This same conclusion applies at e^+e^- colliders, where clear jet structure becomes apparent only for $W > 25 \text{ GeV}$.¹⁵
4. There is a need for high luminosity (hadron) colliders at $\sqrt{s} \sim 1 \text{ TeV}$ to open up phase space for QCD subprocesses, $\sqrt{s} \sim 300 \text{ GeV}$.
5. Ten TeV and 40 TeV colliders need luminosities much greater than $10^{30} \text{ cm}^{-2} \text{ sec}^{-1}$ to overcome the $\alpha_s^2(Q^2)/Q^4$ damping of gluon exchange to get to higher momentum-transfers $Q \sim 1 \text{ TeV}$.
6. It would be nice to see physics results at $\sqrt{s} \sim 1 \text{ TeV}$, where there will certainly be surprises, before prognosticating at $\sqrt{s} = 10$ to 40 TeV.

References

1. S.D. Drell, *Annals of Physics* 4, 75 (1958); S. Brodsky & S. Drell, *Ann. Rev. Nucl. Sci.* 20, 147 (1970).
2. R. Cutler & D. Sivers, *Phys. Rev.* D16, 679 (1977); D17, 196 (1978).
3. B.L. Combridge, J. Kripfganz & J. Ranft, *Phys. Lett.* 70B, 234 (1977).
4. P. Darriulat, et. al., *Nucl. Phys.* B107, 429 (1976); M. Della Negra et. al., *Nucl. Phys.* B127, 1 (1977).
5. R. Feynman, R. Field & G. Fox, *Nucl. Phys.* B128, 1 (1977).
6. A.L.S. Angelis, et. al., *Physica Scripta* 19, 116 (1979); *Physics Letters* 97B, 163 (1980).
7. E. Berger & S. Brodsky, *Phys. Rev. Letters* 42, 940 (1979).
8. 1979 Lepton-Photon Symposium at Fermilab, Section I, any paper.
9. C. Bromberg, et. al., *Phys. Rev. Letters* 43, 565 (1979).
10. C. Bromberg, et. al., *Nucl. Phys.* B134, 189 (1978).
11. See also M. Binkley et. al., *Phys. Rev. Letters* 37, 571 (1976); D.C. Hom et. al., *ibid.* 1374 (1976).
12. W. Bartel et. al., *Phys. Lett.* 101B, 129 (1981).
13. H.J. Behrend et. al., Preprint D Ph PE 82-08, contribution #555 submitted to XXI International Conference High Energy Physics, Paris 1982.
14. R.D. Field & S. Wolfram, preprint CALT 68-909, UFTP82-12, Jan. 1982, and references therein.
15. P. Soding, "Evidence on the Gluon", *Particles and Fields 1981*, Santa Cruz, AIP Conference Proceedings #81.
16. Finjord et. al., *Phys. Letters* 112B, 489 (1982); see also E. Berger & D. Jones, *Phys. Rev.* D23, 1521 (1981).
17. J. Ellis and I. Karliner, *Nucl. Phys.* B148, 141 (1979).
18. F. Paige & I. Stumer, Proc. ISABELLE Summer Study 1981 (BNL-51443, Brookhaven National Laboratory, Upton, NY, 1981), p. 479.
19. B.L. Combridge, *Nucl. Phys.* B174, 243 (1980).
20. A. DeVoto, et. al., *Phys. Rev. Letters*, 43, 1062 (1979).
21. T.L. Trueman, private communication.
22. G.P. LePage & S.J. Brodsky, *Phys. Rev.* D22, 2157 (1980).
23. M.J. Tannenbaum, D.P.F., Montreal, 1979.
24. P. Darriulat, *Ann. Rev. of Nucl. and Particle Science*, 30, 159 (1980).
25. H.G. Fischer, E.P.S., Lisbon 1981.
26. D. Haidt, I. Maneili, *Electron-Photon*, Bonn 1981.
27. M. Jacob and P. Landshoff, *Phys. Rep.* 48C, 285 (1978).
28. A.L.S. Angelis, et. al., CERN-EP/82-133, to be published in *Nuclear Physics B*.
29. R.F. Cahalan, et. al., *Phys. Rev.* D11, 1199 (1975).
30. A.L.S. Angelis, et. al., *Phys. Lett.* 79B, 505 (1978).
31. F. Paige, 1981 ISABELLE Summer Workshop (unpublished), and private communication.
32. J.F. Owens, et. al., *Phys. Rev.* D18, 1501 (1978).
33. R.L. Cool, Presented at this meeting.
34. H. Sticker, Rockefeller Univ. Report DOE/ER/400 33-25, 1982.
35. G. Bordes and A. Nicolaidis, *Phys. Rev.* D22, 2152 (1980); *Phys. Lett.* 114B, 175 (1982).
36. e.g., See R.J. Hollebeek in *Proceedings of Electron-Photon*, Bonn. 1981.
37. See also Field & Feynman *Nucl. Phys.* B136, 1 (1978).
38. UA1 Collaboration, G. Arnison et. al., *Phys. Lett.* 107B, 320 (1981).
39. B. Brown et. al., *Phys. Rev. Letters* 49, 711 (1982).
40. UA2 Collaboration, J-P Repellin, *International Conference on High Energy Physics*, Paris 1982.

Acknowledgment

I would like to thank Pamela M. Brown for typing this paper.